

The build-up of halos within Press-Schechter theory

Will J. Percival

Institute for Astronomy, University of Edinburgh, Royal Observatory, Blackford Hill, Edinburgh EH9 3HJ, U.K.

Submitted for publication in MNRAS

ABSTRACT

Modelling the build-up of halos is important for linking the formation of galaxies with cosmological models. A simple model of halo growth is provided by Press-Schechter (PS) theory, where the initial field of density fluctuations is smoothed using spherically symmetric filters centred on a given position to obtain information about the likelihood of later collapse on varying scales. In this paper the predicted halo mass growth is compared for three filter shapes: Gaussian, top-hat and sharp k -space. Preliminary work is also presented analysing the build-up of halos within numerical simulations using a friends-of-friends group finder. The best-fit to the simulation mass function was obtained using PS theory with a top-hat filter. By comparing both the backwards conditional mass function, which gives the distribution of halo progenitors, and the distribution of halo mergers in time, the build-up of halos in the simulations is shown to be better fitted by PS theory with a sharp k -space filter. This strengthens previous work, which also found the build-up of halos in simulations to be well matched to PS theory with a sharp k -space filter by providing a direct comparison of different filters and by extending the statistical tools used to analyse halo mass growth. The usefulness of this work is illustrated by showing that the cosmological evolution in the proportion of halos that have undergone recent merger is predicted to be independent of mass and power spectrum and to only depend upon cosmology. Recent results from observations of field galaxies are shown to match the evolution expected, but are not sufficiently accurate to usefully distinguish between cosmological parameters.

Key words: galaxies:formation, galaxies:halos, galaxies:evolution, cosmology:theory, cosmology:dark matter

1 INTRODUCTION

Deep surveys are beginning to probe the morphological evolution of non-active field galaxies out to redshifts where cosmological changes in the population as a whole become apparent. The evolution of such galaxies is expected to be driven by the hierarchical build-up of the dark matter halos in which the galaxies reside, with mergers between halos of approximately equal size being particularly important. Such mergers can lead to the disruption of galaxy structure producing observable signatures. Consequently, it is important to be able to model the growth of halos in sufficient detail to determine the relative frequency of mergers.

Press-Schechter (PS) theory (Press & Schechter 1974) provides a simple analytic model for the build-up of halos. In this theory, the initial field of density fluctuations is smoothed on varying scales around a given position to obtain information about the probability of later collapse. The distribution of overdensities as a function of filter size is called a trajectory. If filter size and halo mass are linked, each trajectory contains information about the mass of halo

within which a test-particle associated with that trajectory and position in the linear density field resides. Linking perturbation amplitude with the epoch at which fluctuations undergo non-linear collapse, and assuming that collapse occurs on the largest scale for which there is sufficient excess overdensity provides a complete model for halo mass growth.

The standard use of PS theory is to calculate the mass function $f(M|t) dM$, the distribution of mass in isolated halos at a given epoch (Press & Schechter 1974; Peacock & Heavens 1990; Bond *et al.* 1991). For the sharp k -space filter, it is possible to obtain an analytic formula, although this is not true for more general filters. A numerical method for generating trajectories for general spherically symmetric filters was given by Bond *et al.* (1991) and is summarized in Section 2. The effect of the choice of filter on the resulting mass function is considered in Section 4, where the top-hat filter is shown to provide the best match to recent N-body simulation results. The distribution of times at which halos of a given mass are created can also be determined by PS theory (Percival & Miller 1999), and is discussed for different filters in Section 5.

It is possible to use PS theory to follow the build-up of halos that have mass M at time t by considering the behaviour of trajectories that pass through this location. This is often called ‘extended PS theory’ and leads to conditional analogues of the mass function and halo creation rate (Bower 1991; Bond *et al.* 1991; Lacey & Cole 1993; Percival & Miller 1999). Extended PS theory is often used to estimate halo merger trees, which are in turn used in semi-analytic models of galaxy formation (Kauffmann & White 1993; Sheth & Lemson 1999; Somerville *et al.* 2000). The distribution of progenitor masses at an earlier epoch is termed the backwards conditional mass function, while the distribution of halo masses in which a particle might find itself at a later time is termed the forward conditional mass function. Lacey & Cole (1994) showed that the forward conditional mass function from simulations with power law spectra appears to be well fitted by a variant of PS theory. In this paper this work is extended to determine the effect of filter choice on the backwards conditional mass function and the predicted frequency of merger events as a mechanism for the build-up of dark matter halos. The backwards mass function is analysed in Section 6. Starting with the premise that mergers between halos correspond to jumps in the mass associated with a single trajectory in PS theory, the relative frequency of mergers are compared for different filters in Section 7.

The usefulness of this analysis is demonstrated in Section 8, where the proportion of halos that have undergone recent merger is calculated. This is linked to the field galaxy merger rate, and recent observational results are shown to be consistent with a variety of cosmological models. Further observations could, in principle, lead to estimates of Ω_m and Ω_v .

2 THE PRINCIPLES OF PRESS-SCHECHTER THEORY

Press-Schechter (PS) theory is based on two simple ideas. First, the field of initial density fluctuations is filtered to determine the amplitude of the perturbations on different scales. Second, the perturbation amplitudes are linked to their collapse time or lack of it, thereby providing a complete statistical model for the build-up of structure in the Universe. Three filters are compared in this paper, defined in k -space by

Sharp k -space

$$\tilde{W}_{ks}(k; R_{ks}) = \vartheta(1 - kR_{ks}) \quad (1)$$

Top-Hat

$$\tilde{W}_{th}(k; R_{th}) = 3 \frac{\sin(kR_{th}) - (kR_{th}) \cos(kR_{th})}{(kR_{th})^3} \quad (2)$$

Gaussian

$$\tilde{W}_g(k; R_g) = \exp\left(\frac{-R_g^2 k^2}{2}\right) \quad (3)$$

where $\vartheta(x)$ is the Heaviside step function, $\vartheta(x) = 1$ for $x \geq 0$ and $\vartheta(x) = 0$ otherwise. The mass variance, σ_M^2 inside a volume V whose shape and size are dependent on the filter is given by

$$\sigma_M^2 = \frac{1}{2\pi^2} \int_0^\infty P(k) \tilde{W}^2(k; R) k^2 dk, \quad (4)$$

where $P(k)$ is the power spectrum of the initial density perturbations, and is often simply referred to as the power spectrum. Unless stated otherwise, the standard CDM power spectrum of Bond *et al.* (1991) has been assumed with $\Gamma \equiv \Omega_m h = 0.5$. The set of overdensities corresponding to different R for a given position in the linear density field (this can also be thought of as corresponding to a test-particle or small mass element) is called a trajectory.

Examples of trajectories created for the filters defined by Equations 1, 2 & 3 are presented in Fig. 1. These trajectories were calculated using Langevin integration as described by Bond *et al.* (1991). First, a Monte-Carlo realisation of a Gaussian random field was created, integrated over contiguous spherical shells in k -space. The amplitudes of the field integrated over non-overlapping shells are independent and, for thin shells from $\ln k \rightarrow \ln k + \delta \ln k$, are given by a Gaussian random variable with variance

$$\sigma_{\text{shell}}^2 = \frac{1}{2\pi^2} k^3 P(k) \delta \ln k. \quad (5)$$

For the trajectories presented in Sections 4 & 5, the field was determined around a given position for 2^{12} shells equally spaced in $-7 < \ln k < 6$. Trajectories were then created by summing over these shells, weighted by the filter window function for 2^8 radii equally spaced in $\log \sigma_M^2$. As a check that the density field is adequately sampled, results are presented in Sections 4 & 5 for the sharp k -space filter, for which the result is known analytically. Tests have also shown that increasing or decreasing the sampling does not significantly alter the results. A detailed analysis of the sampling required to calculate the backwards conditional mass function is given in Section 6.

In order to provide a complete description of the hierarchical build-up of mass, the epoch of collapse must be linked with the overdensity. In fact, the link between the critical overdensity δ_c and the collapse epoch is predicted to be independent of mass for the simple spherical top-hat collapse model (Percival, Miller & Peacock 2000), the model adopted in standard PS theory. The mass of halo surrounding a given position at time t is then given by the first, or largest mass, upcrossing of a horizontal barrier $\delta = \delta_c(t)$ by the trajectory.

3 PARAMETERS IN PS THEORY

This Section discusses the free parameters in Press-Schechter theory, and outlines the conventions used in this paper.

The choice of filter was presented as a single free parameter in Section 2. However, because PS theory only predicts an analytic form for the unconditional and conditional mass functions for the sharp k -space filter, many authors have in the past used these analytic functions and have calculated σ_M^2 using a different filter. The choice of filter used to calculate σ_M^2 becomes an additional free parameter in PS theory (with the choice of filter to determine the mass function being a different free parameter). For instance, both Kauffmann & White (1993) and Somerville & Kolatt (1999) use the spatial top-hat filter to calculate σ_M^2 , and the sharp k -

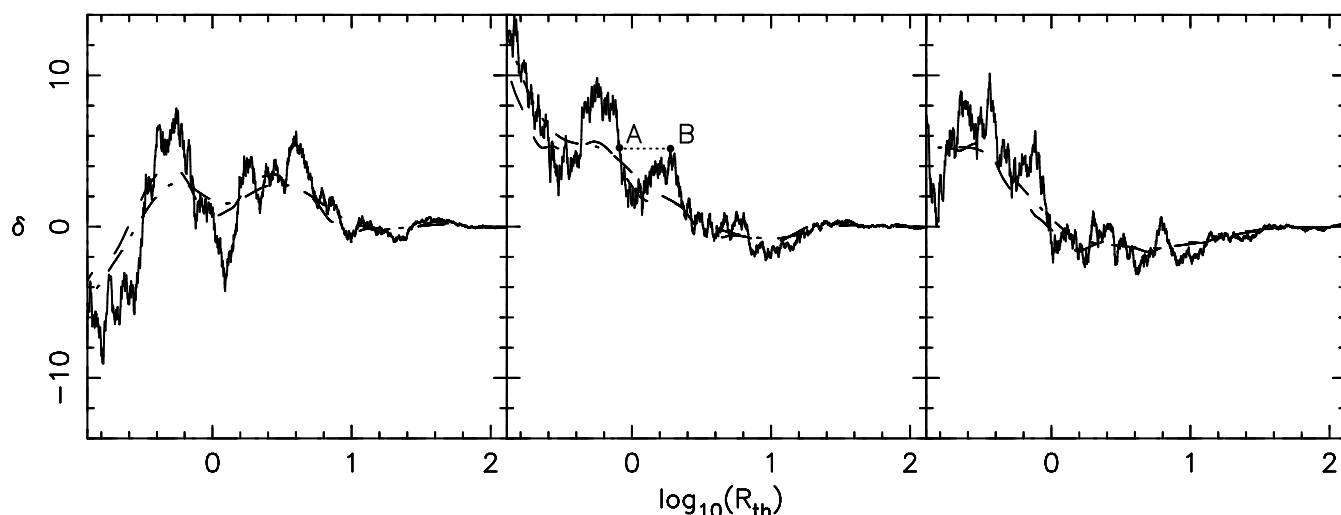


Figure 1. Trajectories are plotted calculated by Langevin integration for three independent positions in a Gaussian random field with CDM power spectrum. For each position, an estimate of the density field was made integrated over 2^{16} contiguous shells equally spaced in $\ln k$. Each Monte-Carlo realisation of the field was then filtered with sharp k -space (solid line), top-hat (dashed line) and Gaussian (dot-dash line) filters at 2^{12} radii, equally spaced in $\log \sigma_M^2$. The top-hat and Gaussian filters provide smoother trajectories than the sharp k -space filter for the same field position although, as expected, the overall behaviour is similar for all filters. Trajectories are matched as described in Section 3. The mass associated with the sharp k -space trajectory shown in the centre panel will undergo a jump from a value corresponding to R_A to a value corresponding to R_B at a time when $\delta_c = \delta_{AB}$, the value along the dotted line.

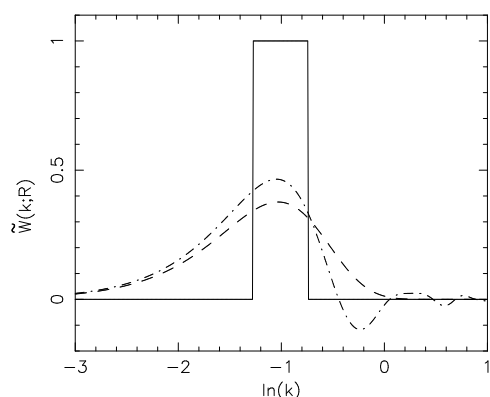


Figure 2. The transitional weighting applied to the k -shells for one step in a trajectory for the sharp k -space (solid line), top-hat (dashed line) and Gaussian (dot-dash line) filters for a change in mass of between 10^{14} and $5 \times 10^{14} M_\odot$. The filters have been matched so that the transitional weighting peaks at the same value of $\ln k$, as described in Section 3.

space filter to determine the mass functions. Similarly, Lacey & Cole (1994), allowed the choice of filter used to calculate σ_M^2 to be different to the sharp k -space filter used to determine the mass function. The effect of this switch is equivalent to using the sharp k -space filter throughout with a slightly modified power spectrum. In this paper, the same filter is used to determine both the mass function and σ_M^2 .

Another parameter that is often allowed to vary is the critical overdensity for collapse, δ_c , with authors tuning this parameter to fit simulations (Lacey & Cole 1994), or using the ellipsoidal collapse model (Sheth, Mo & Tormen 2001). For simplicity, only the spherical top-hat collapse model is considered in this paper.

In order to compare results calculated using different

filters, the radii of the different filters need to be matched. In each step of a trajectory, the power spectrum is convolved with a transitional weighting function. Fig. 2 shows an example of the transitional weighting applied by the three filters considered in this paper. Matching the radii of the different filters effectively matches the weightings applied to the power spectrum. A common method is to integrate each filter over all real space to calculate its ‘volume of influence’ and the average mass enclosed. Equating volumes leads to

$$R_{ks} = \left(\frac{9\pi}{2}\right)^{-1/3} R_{th} \simeq 0.414 R_{th}, \quad (6)$$

$$R_g = \left(\frac{4\pi}{3}\right)^{1/3} \frac{1}{(2\pi)^{1/2}} R_{th} \simeq 0.643 R_{th}. \quad (7)$$

For the differentiable filters it is also possible to match filter radii to second order in the expansion around $k = 0$. This requires $R_g = 1/\sqrt{5} R_{th} \simeq 0.447 R_{th}$.

Each point in a trajectory is calculated by integrating over k -shells, and matching different filters simply alters the region of the power spectrum probed. It is possible to directly match the peak value of k probed at a given step in a trajectory. For the non-differentiable sharp k -space filter, $k_{\max} = 1/R_{ks}$. For the Gaussian filter the first solution to the differential equation $d^2\tilde{W}/dRdk = 0$ is given by $k_{\max} = \sqrt{2}/R_g$ and for the top-hat filter solving this equation numerically gives $k_{\max} \simeq 3.342/R_{th}$. Combining these equations gives

$$R_{ks} \simeq 0.299 R_{th}, \quad R_g \simeq 0.423 R_{th}. \quad (8)$$

The differential weighting applied in a particular trajectory ‘step’ by each filter for this choice of matching filters is shown in Fig. 2.

In order to highlight the effect of filter choice on halo growth, it seems prudent to ensure that the same region of the power spectrum is probed at each trajectory step.

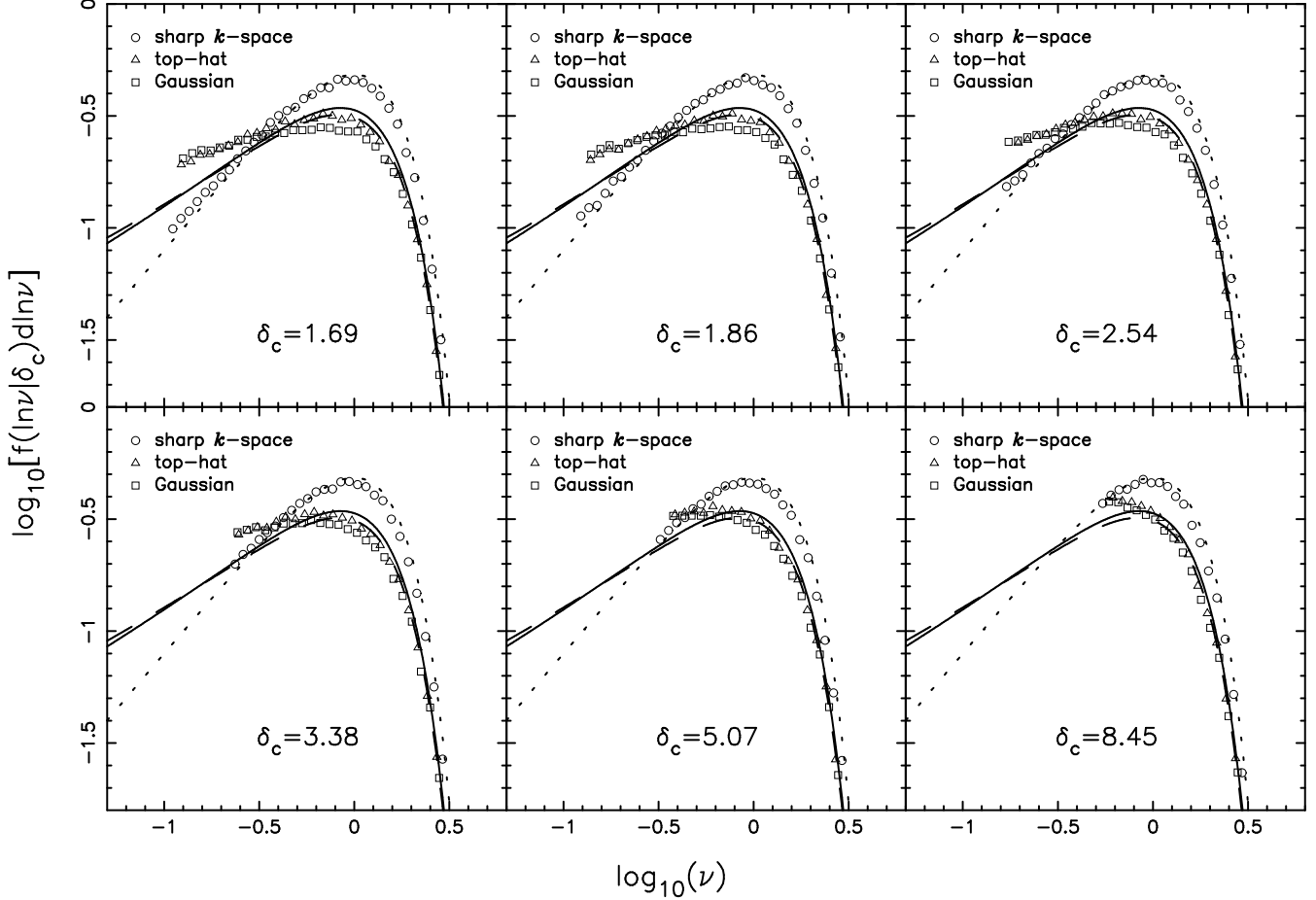


Figure 3. The halo mass function is presented for each filter as a function of $\nu \equiv \delta_c/\sigma_M$ for six values of δ_c , calculated from 10^6 Monte-Carlo trajectories. The six values of δ_c correspond to redshifts of 0.0, 0.1, 0.5, 1.0, 2.0 and 4.0 for an Einstein-de Sitter cosmology. The prediction of PS theory for a sharp k -space filter is also plotted (dotted line), and is a close match to the corresponding numerical data. The slight deviation is caused by differing sampling of the field and trajectory. Because of the filter shapes, such a difference will affect results for the top-hat & Gaussian filters less. Results for different filters were matched as described in Section 3. The dashed line shows the fit to N-body simulation results of Sheth & Tormen (1999), and the solid line the fit of Percival *et al.* (2000).

Because of this, where appropriate, the filter radii have been matched using Equation 8. Having adopted this convention, the halo mass M was defined as

$$M = \frac{4\pi}{3} \bar{\rho} R_{th}^3, \quad (9)$$

where $\bar{\rho}$ is the mean density of the universe. Because the mass variance, σ_M^2 is dependent on filter choice (Equation 4), comparing results as a function of σ_M^2 implicitly matches filter radii. In this case, the relationship between the radii of different filters is dependent on the power spectrum. Filter radii are only matched using Equation 8 when the halo mass is required.

4 THE HALO MASS FUNCTION

The mass function $f(M|t) dM$, gives the distribution of mass in isolated halos at a given epoch, and is related to the number density of halos by $\bar{\rho} f(M|t) dM = Mn(M) dM$. The mass function can be calculated analytically for a sharp k -space filter because the trajectories are Brownian random walks and therefore have special symmetries (Press &

Schechter 1974; Peacock & Heavens 1990; Bond *et al.* 1991). Defining

$$\nu \equiv \frac{\delta_c}{\sigma_M}, \quad (10)$$

the PS mass function can be written as

$$f(\ln \nu|t) d \ln \nu = \sqrt{\frac{2}{\pi}} \nu e^{-\nu^2/2} d \ln \nu. \quad (11)$$

Note that when the mass function is written in this way, its form is independent of epoch. It is not possible to obtain corresponding analytic formulae for top-hat or Gaussian filtering (Bond *et al.* 1991).

By creating an ensemble of 10^6 trajectories for each of the filters given by Equations 1, 2 & 3 using the method described in Section 2, the mass function has been estimated at six epochs. These data are presented in Fig. 3 as a function of ν .

Recent work analysing the mass function predicted by numerical simulations has suggested that, although the mass function has a universal form when written as a function of ν , this form is altered from that of Equation 11 (Sheth

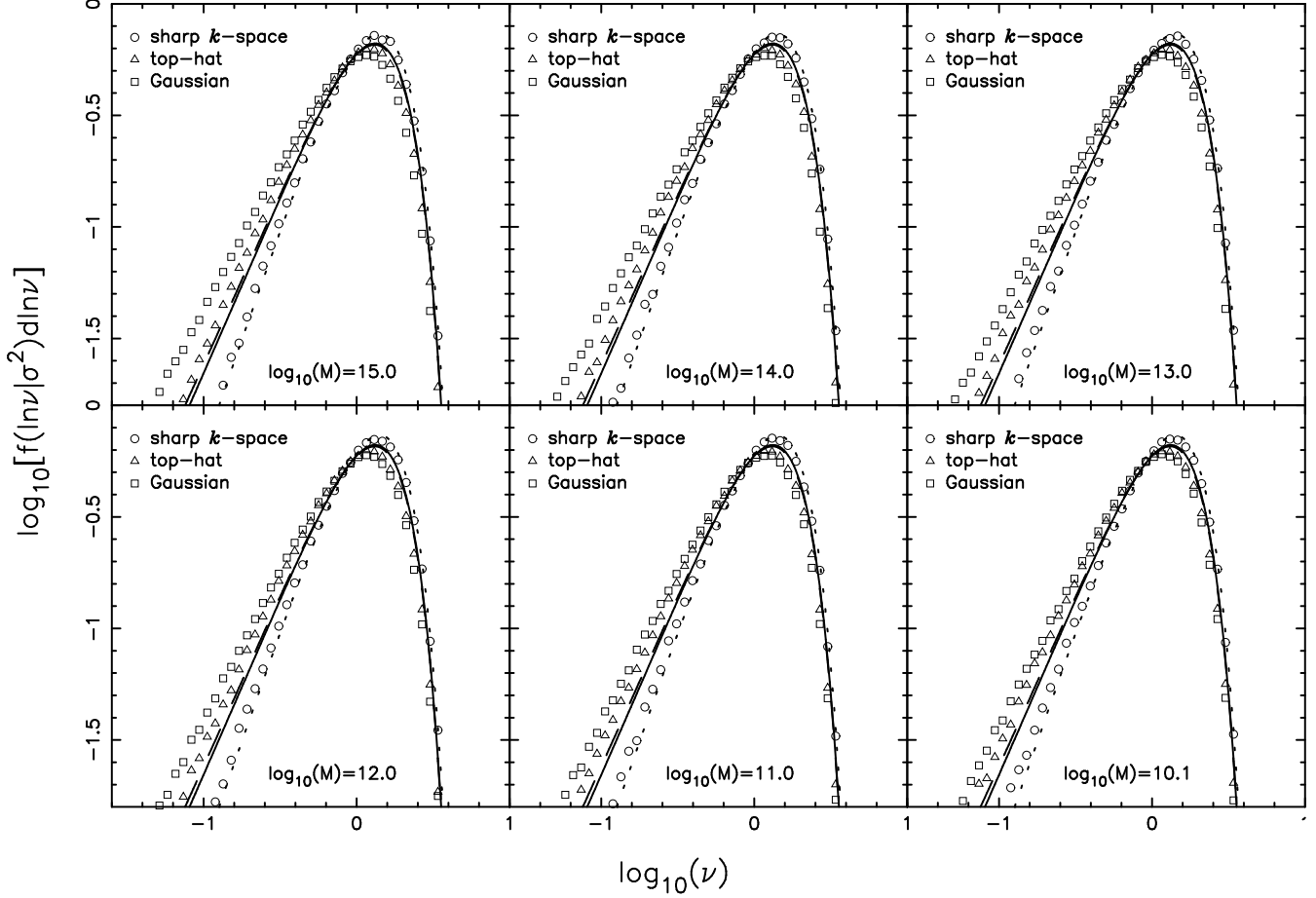


Figure 4. The distribution of halo creation times are plotted for six halo masses as a function of $\nu \equiv \delta_c/\sigma_M$. These data were calculated from 10^6 Monte-Carlo trajectories created as described in Section 2. The lines are as in Fig. 3, converted into creation rates by multiplying by ν (Percival, *et al.* 2000). The Monte-Carlo data have been normalized to the model of Sheth & Tormen (1999).

& Tormen 1999; Percival, *et al.* 2000; Jenkins *et al.* 2001). Instead, Sheth & Tormen (1999) found that a good fit to the N-body data was given by

$$f(\ln \nu|t) d \ln \nu = A \sqrt{\frac{2}{\pi}} \left(1 + \frac{1}{\nu'^{2p}}\right) \nu' e^{-\nu'^2/2} d \ln \nu, \quad (12)$$

where $\nu' = a^{1/2} \nu$ and a & p are parameters. A is determined by requiring that the probability density function is correctly normalized. Sheth & Tormen found best fit parameters $a = 0.707$ and $p = 0.3$ for their simulations and group finding algorithm. The standard PS multiplicity function has $a = 1$, $p = 0$ and $A = 1/2$. In Percival *et al.* (2000), a small tweak was required for the parameters in order to fit the data giving $a = 0.774$ & $p = 0.274$. These fits to the mass function are presented in Fig. 3.

The mass function calculated from trajectories determined for the sharp k -space has close to its predicted analytic behaviour given by Equation 11, showing that the Monte-Carlo procedure works for this filter. The smoother trajectories calculated for the top-hat and Gaussian filters produce mass functions more like that observed in numerical simulations, with fewer high mass halos than predicted by Equation 11. This match is not perfect, and the smoother filters predict more low mass halos than Equation 12.

5 THE HALO CREATION RATE

The halo creation rate $f(t|M) dt$ for halos of mass M is given by the distribution of first upcrossing times of a barrier at the filter radius corresponding to M . The distribution of halo creation times determined for Gaussian, top-hat and sharp k -space filters are plotted in Fig. 4 for the subset of Monte-Carlo trajectories that predict the creation of a halo with one of six masses. Each trajectory does not necessarily have a first upcrossing at a particular mass because the mass can undergo finite ‘jumps’ (see Section 7). Consequently, the total number of creation events recorded from a fixed number of trajectories depends on the filter chosen. As the sharp k -space filter provides a ‘rough’ trajectory compared to top-hat and Gaussian, there are more mass jumps and less creation events for this filter at a given final halo mass. In fact, it is only because of the discrete nature of these trajectories that any creation events at a particular mass are found.

It follows from the Bayesian argument presented in Percival *et al.* (2000) that

$$\nu f(\ln \nu|t) d \ln \nu \propto f(\ln \nu|M) d \ln \nu. \quad (13)$$

In the first of these probability density functions ν is considered to be a function of mass, while in the second it is

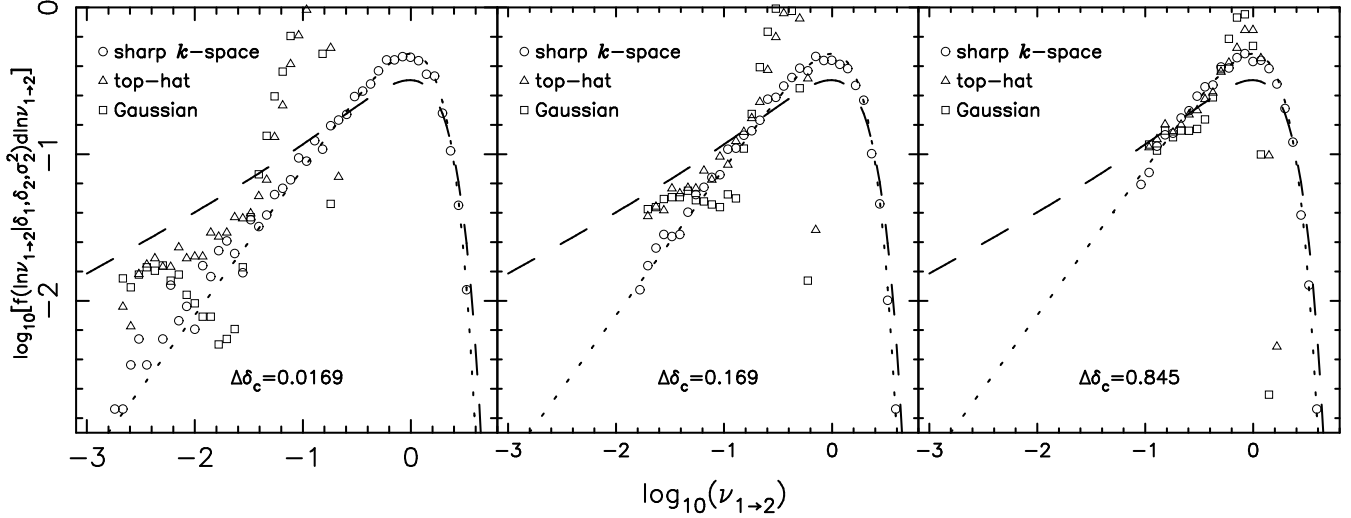


Figure 5. The backwards conditional mass function calculated for PS theory with three filters is presented as a function of $\nu_{1 \rightarrow 2}$, for σ_2^2 equivalent to a mass of $10^{14} M_\odot$. All trajectories that predict a halo of mass $10^{14} M_\odot$ at $\delta_2 > 1.69$ were included in this analysis. The dotted line shows the analytic prediction of PS theory with a sharp k -space filter, and the dashed line shows the fit to the mass function of Sheth & Tormen (1999), presented as if its form is invariant to the change $\nu \rightarrow \nu_{1 \rightarrow 2}$.

considered to be a function of time. The model mass functions plotted in Fig. 3 have been converted to creation rates by multiplying by ν and renormalising, and are compared with the creation rate calculated from the Monte-Carlo trajectories in Fig. 4.

The results are similar to those of Fig. 3, with the Monte-Carlo creation rate calculated for the sharp k -space filter closely following the expected form. The creation rates calculated using the fit to the N-body simulations (Equation 12) are closer to PS theory with the top-hat and Gaussian filters although, as for the mass function, the match is not perfect. Comparing Figs. 3 & 4 shows that the Bayesian link between the halo creation rate and mass function is closely followed by the Monte-Carlo data.

6 THE BACKWARDS CONDITIONAL MASS FUNCTION

6.1 PS theory

The subset of trajectories that pass through a selected position determine the probability density functions for the past and future masses of that halo. As for the mass function, analytic formulae are possible for the sharp k -space filter (Bower 1991; Bond *et al.* 1991; Lacey & Cole 1993), whereas for top-hat and Gaussian filters numerical techniques must be used. The conditional analogue of ν is defined as

$$\nu_{1 \rightarrow 2} \equiv \frac{\delta_1 - \delta_2}{\sqrt{\sigma_1^2 - \sigma_2^2}}, \quad (14)$$

where $\sigma_2^2 < \sigma_1^2$ ($M_2 > M_1$) and $\delta_2 < \delta_1$ ($t_2 > t_1$), and the subscripts M and c have been omitted for simplicity. For the backwards conditional mass function, σ_2^2 and δ_2 (and δ_1) are known and $\nu_{1 \rightarrow 2}$ is considered to be a function of σ_1^2 . For the sharp k -space filter

$$f(\ln \nu_{1 \rightarrow 2} | \delta_1, \delta_2, \sigma_2^2) d \ln \nu_{1 \rightarrow 2}$$

$$= \sqrt{\frac{2}{\pi}} \nu_{1 \rightarrow 2} e^{-\nu_{1 \rightarrow 2}^2/2} d \ln \nu_{1 \rightarrow 2}, \quad (15)$$

which has the same form as Equation 11. This is expected because the form of the trajectories is invariant to a linear shift in δ or σ^2 .

For the top-hat and Gaussian filters, the equivalent distribution can be calculated by analysing numerical realisations of trajectories. In order that all upcrossings at small $\Delta \delta_c \equiv (\delta_2 - \delta_1)$ were realized, the trajectories used for this analysis were sampled at 2^{10} steps in R , equally spaced in $-6 < \log_{10}(\sigma_2^2 - \sigma_1^2) < 2$. For the sharp k -space filter, only a single k -shell covering each interval in R is required. The other two filters have a broader shape and each step in a trajectory will depend on a larger region of k -space. Two k -shells within each interval in R and 2^7 shells either side of the minimum and maximum radii, equally spaced in $\ln k$ were found to sufficiently sample k -space.

The backwards conditional mass functions resulting from these trajectories are presented in Fig. 5 for three values of $\Delta \delta_c$. In order to match the N-body results (for an Einstein-de Sitter cosmology), only trajectories that predict a halo of mass $10^{14} M_\odot$ at $\delta_1 > 1.69$ have been counted. The smoother trajectories calculated using top-hat and Gaussian filters predict low mass progenitors, particularly for small $\Delta \delta_c$.

6.2 Numerical Simulations

Three numerical simulations, completed using the Hydra N-body, hydrodynamics code (Couchman, Thomas & Pearce 1995), have been analysed in order to estimate the backwards conditional mass function for halos of mass $\sim 10^{14} M_\odot$. Details of the cosmologies adopted for these simulations are summarized in Table 1. Each simulation contained 128^3 dark matter particles, and particle positions were output at a large number of epochs (362 for Λ CDM, 345 for Ω CDM & 499 for Λ CDM), separated by approx-

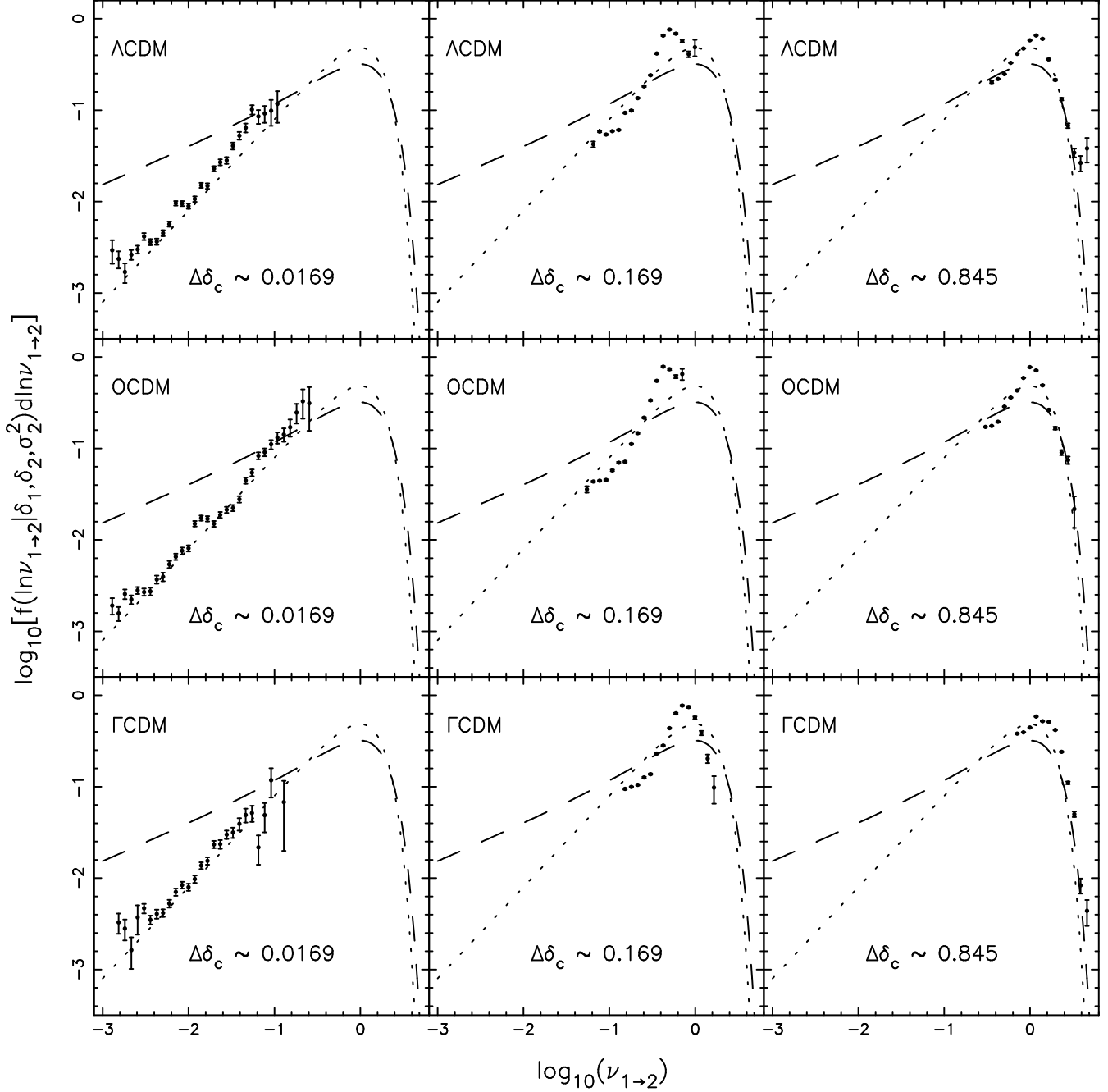


Figure 6. The backward conditional mass function calculated from three N-body simulations (See text for details). The left column shows the backwards conditional mass function from consecutive output from the simulation, while the centre column shows the backward conditional mass function for $\Delta\delta_c \sim 0.169$, and the right column $\Delta\delta_c \sim 0.845$. The rows show results from different simulations. Lines are plotted as in Fig. 5.

| model | Ω_M | Ω_V | Γ | σ_8 | h |
|---------------|------------|------------|----------|------------|-----|
| Γ CDM | 1 | 0 | 0.25 | 0.64 | 0.5 |
| OCDM | 0.3 | 0 | 0.15 | 0.85 | 0.5 |
| Λ CDM | 0.3 | 0.7 | 0.15 | 0.85 | 0.5 |

Table 1. Table showing the parameters of the cosmological models adopted in the three N-body simulations.

imately equal intervals in time. The box size chosen was $100 h^{-1} \text{Mpc}$ for all three simulations that gave a particle

mass of $2.6 \times 10^{11} M_\odot$ for Γ CDM and $7.9 \times 10^{10} M_\odot$ for the other two simulations. Groups of particles were found using a standard friends-of-friends algorithm with linking length set to $b = 0.2$ times the mean interparticle separation.

Fig. 6 shows the conditional mass function calculated for different values of $\Delta\delta_c$. Halos of between 200 and 1500 particles were selected from every output time, corresponding to masses $1.6 \times 10^{13} M_\odot < M < 3.9 \times 10^{14} M_\odot$, and the particles were traced back to determine the mass of the halo they resided in at the output time nearest the required $\Delta\delta_c$.

Only halos containing at least 40 particles, and with over 50% of their particles in common with the final halo were considered to be progenitors. The choice of 50% is reasonably arbitrary, and does not affect the progenitor distribution significantly. σ_M^2 was calculated for these halos using the top-hat filter. We have tried using Gaussian and sharp k -space filters to calculate σ_M^2 and find that the result is not significantly affected by this choice.

The values of $\Delta\delta_c$ adopted correspond to $\Delta z \sim 0.01$, $\Delta z = 0.1$ and $\Delta z = 0.5$ for an Einstein-de Sitter cosmology. The smallest of these intervals corresponds to consecutive output from the simulations.

Comparing Fig. 5 and Fig. 6 provides weak evidence that the build-up of halos in PS theory is most like that predicted by the sharp k -space filter. This is discussed further in Section 9.

7 THE COSMOLOGICAL DISTRIBUTION OF MERGERS

In order to link halo growth with the observed evolution of the baryonic component of galaxies, it is important to distinguish between major mergers, which can disrupt structure creating observable signatures, and the slow accretion of matter. Where trajectories dip and rise again (as the filter radius decreases), the mass associated with the trajectory undergoes a jump. Such an event is shown in Fig. 1 for a trajectory calculated with a sharp k -space filter. These jumps are often associated with mergers, and it is expected that close congregations of excess overdensity in the linear density field that initially collapse as single entities and subsequently merge together, will create such a dip and rise as the filter increases in size and the number of enclosed clumps increases. For PS theory with a sharp k -space filter, jumps are the only mechanism for gaining mass as the trajectories are not differentiable.

The halo creation events analysed in this Section can be thought of as being instantaneous. However, numerical limitations are placed on how well we can follow these events because the trajectories are discretized in mass and the simulations are discretized in both mass and time. For the simulations, simultaneous outputs from the simulations were used to determine whether a halo had just been created, and whether the creation event was a merger. For the trajectories, the behaviour of a trajectory before it passed through a point was analysed to determine whether it was a first up-crossing (a creation event), and the subsequent behaviour was analysed to determine the form of creation. Both the trajectories and the simulations were sufficiently sampled that this numerical problem should not affect the conclusions drawn from this work. Defining the merger fraction, $f_{\text{merg}}(M_f, z_f)$, by

$$f_{\text{merg}}(M_f, z_f) = \frac{\text{No. mergers}}{\text{No. new halos}} \Big|_{M_f, z_f}, \quad (16)$$

where z_f is the final redshift of the halo and M_f is the final mass of the halo, we can write the normalized proportion of new halos created by merger as

$$\mu'(M_f, z_f) = \frac{f_{\text{merg}}(M_f, z_f)}{\bar{f}_{\text{merg}}(M_f)} \quad (17)$$

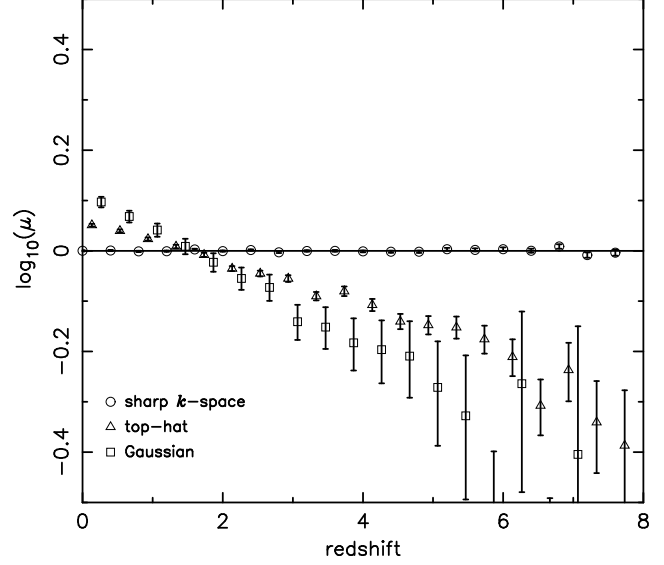


Figure 7. The normalized proportion of halo creation events that are a result of merger, measured from a set of 10^6 trajectories, calculated for each of the three filters described by Equations 1 - 3. Here, a merger was defined to be a mass jump of at least a quarter of the final mass, with the trajectory after the jump also corresponding to a halo with mass over a quarter of the final value.

where $\bar{f}_{\text{merg}}(M_f)$ is the average of $f_{\text{merg}}(M_f, z_f)$ over all redshift. These data were combined over all final halo masses of interest, weighted by the standard Binomial variance treating the number of creation events found for each M_f and z_f as the number of ‘experiments’ performed. The resulting normalized merger fraction, a function of redshift only, is denoted by μ . This procedure is designed to allow the merger fraction to be a function of mass and to highlight any cosmological changes in the overall merger rate.

Fig. 7 shows the cosmological variation in μ , calculated from PS trajectories, for mergers defined such that both the mass jump and the progenitor correspond to at least a quarter of the mass of the final halo. Results presented in this Section are not sensitive to this choice. The numbers of mergers and halo creation events were determined from a set of 10^6 trajectories, calculated as described in Section 2 for each of the three filters given by Equations 1 - 3. The discrete nature of the trajectories provides the required lower limit of the size of possible accretion event and stops the number of halo creation events in any time interval becoming infinite. Data have been combined for all creation events that result in a halo of mass $4 \times 10^{10} M_\odot < M < 10^{13} M_\odot$, in such a way that the results should be directly comparable with those calculated from N-body simulations.

The Markovian nature of the trajectories calculated using a sharp k -space filter means that the probability that a halo was created by merger is independent of creation time: the normalized merger probability is flat. However, the trajectories calculated for the other filters are non-Markovian and the probability of merger is dependent on cosmological epoch. There is a general trend for these filters that when a halo is created at early times it’s more likely to have been created via the slow build-up of matter rather than by merger.

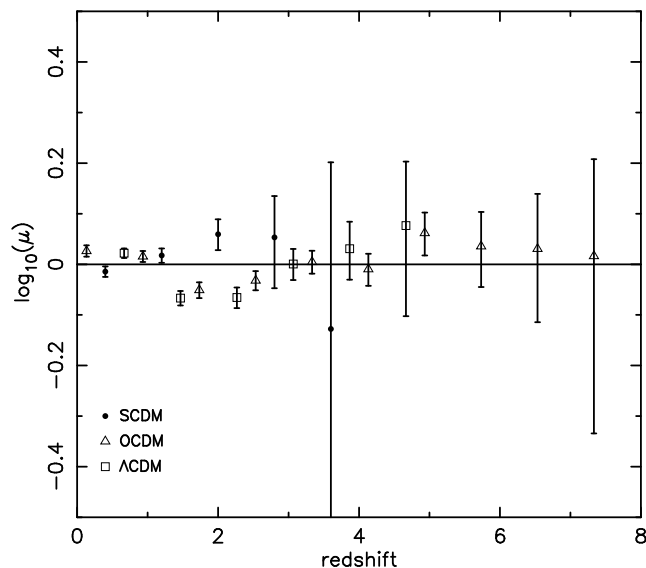


Figure 8. The normalized proportion of halo creation events that are a result of merger, measured from three N-body simulations from which groups of particles were determined using a standard friends-of-friends group finder with $b = 0.2$. Halo creation was defined to have occurred for a given halo at a particular time if at least half of the particles had not previously been contained within a halo with equal or greater mass. Only halos comprising at least 45 particles were included in this analysis. A creation event was said to have been a merger if there were two possible progenitors at the previous output time from the simulation, each with mass greater than a quarter of the final halo mass. The data are not strongly dependent on this choice, and are consistent with no evolution in the proportion of merger events as a means of halo creation.

It is interesting to compare this behaviour with that observed in N-body simulations. Here, the discrete nature of the simulations stops the number of halo creation events within a time interval from tending to infinity. Halo creation was defined to have occurred for a given halo at a given time if at least half of the particles had not previously been contained within a halo with equal or greater mass. Only halos comprising at least 45 particles were included in this analysis. A creation event was said to have been a merger if there were two possible progenitors at the previous output, each with mass greater than a quarter of the final halo mass. Using the analysis described above for combining data from halos of different mass, these data are presented in Fig. 8.

Fig. 8 suggests that the distribution of mergers follows the PS model with a sharp k -space filter, with no evidence for a cosmological trend as predicted by PS theory with either the top-hat or Gaussian filters. PS theory with the sharp k -space filter would therefore seem to provide the best model for the build-up of clumps of dark matter determined using the FOF algorithm.

8 THE TIE-IN WITH OBSERVED GALAXY EVOLUTION

A variety of different techniques have been used to determine the amount of evolution in the field galaxy merger rate as a function of redshift: recent studies have used ob-

servations of the cosmological change in either the angular correlation function (Neuschaefer *et al.* 1997), pair counts (Carlberg, Pritchet & Infante 1994; Patton *et al.* 1997) or galaxy morphologies (Lavery *et al.* 1996). See Abraham *et al.* (1998) for a review. There is now strong evidence that the number of interacting systems grows rapidly with look-back time. The cosmological change in the proportion of galaxies involved in mergers is usually fitted by a power-law of the form $(1+z)^n$, and results are parametrized by the best fit value of n . A recent study using follow-up HST imaging of a sample of 185 galaxies with measured redshifts from the CFRS and Autofib-LDSS surveys has provided the most convincing measurement of n to date (Le Fèvre *et al.* 2000). This work extends the pair-count analysis of Patton *et al.* (1997) from $z = 0.33$ to $z = 0.9$ and reveals a consistent amount of evolution between such studies and results from the morphological classification of galaxies. A best fit value of $n = 2.7 \pm 0.6$ is determined after correction for biases attributed to selection effects: the combination of ground-based and HST observations means that the sample is biased towards finding close pairs that are thought to be single galaxies in the magnitude limited ground-based sample, but which can be resolved into separate galaxies by HST.

These observational studies select galaxies based on properties of the baryonic galaxy component. In order to model such observations, the predicted evolution in the halo merger rate has to be combined with the time-scale over which the tracers of halo merger are visible, including any time difference between the merger of the baryonic components and the halos caused by the dynamical friction time-scale. The dynamical friction time-scale describes how long it takes for a galaxy (or progenitor) to spiral to the centre of a halo. If this takes a long time compared to the cosmological time-scale of interest, it would affect the relative distribution of baryonic and halo mergers. However, by concentrating on galaxies in small groups or field galaxies at relatively low redshifts, the dynamical friction timescale is expected to be small (Barnes & Hernquist 1992). For such studies, or by using galaxy counts rather than morphologies, the observed evolution is expected to be driven by the proportion of halos that have undergone recent merger.

Percival *et al.* (2000) showed that multiplying the mass function by $d\delta_c/dt$ leads to the joint distribution of halo creation events in mass and time. In Section 7 the distribution of mergers in numerical simulations was shown to follow that predicted by PS theory with a sharp k -space filter, and to have the same form as the distribution of creation events. The proportion of halos that have just undergone merger is given by the creation rate divided by the number of halos, given by the standard PS mass function (Equation 11). The resulting cosmological change is proportional to $d\delta_c/dt$, and only depends on the Friedmann equation. A method for calculating $d\delta_c/dt$ was given by Percival *et al.* (2000). Because PS theory does not include sub-halos that form part of a larger collapsed system, this is only valid for field galaxies. This will also be the evolution of any combination of halos of different mass, provided the combination is independent of redshift. For the three cosmologies parametrized in Table 1, approximating $d\delta_c/dt$ by $(1+z)^n$ gives $n = 2.5$ for SCDM, $n = 2.1$ for OCDM and $n = 2.3$ for LCDM. These values are in agreement with the best fit value of Le Fèvre *et al.* (2000), $n = 2.7 \pm 0.6$ within the errors and uncertainties.

Further observations to provide more accurate observational data could, in principle, provide an interesting mechanism for constraining the best-fit cosmology.

9 CONCLUSIONS

The build-up of halos predicted by PS theory has been shown to be strongly dependent on the filter used to smooth the density field. None of the filters provides a perfect match for the build-up of structure in the numerical simulations presented in this paper. The simulation mass function (Sheth & Tormen 1999; Percival, *et al.* 2000) is most similar with PS theory with a top-hat filter, as is the halo creation rate.

The top-hat and Gaussian filters predict mass growth due to continuous accretion with the occasional merger, while the sharp k space filter predicts mass growth completely due to mergers. Because of this, the predicted backwards conditional mass function is strongly dependent on the choice of filter. Analysing numerical simulations suggests a backwards conditional mass function most like that of PS theory with the sharp k -space filter, although again, the match is not perfect. The resolution of the simulations means that it is difficult to resolve mergers with small enough halos. However, there is weak evidence that the simulations contain more mergers with small mass halos than are predicted by the smoother trajectories associated with the top-hat and Gaussian filters.

For the sharp k -space filter, the cosmological distribution of halo mergers is independent of merger parameters. This result follows from the Markovian nature of the trajectories produced. For the other filters, which predict non-Markovian trajectories, the probability of merger is shown to be dependent on the halo creation epoch. No evolution is seen in the probability that a given halo was created by merger measured from N-body simulations, and PS theory with a sharp k -space therefore provides the best fit to these data. This provides the most convincing evidence that PS theory with a sharp k -space filter provides the best model of halo growth. In this work, a standard FOF group finder was used. An interesting test would be to analyse the observed build-up of halos using a number of different algorithms to find halos. However, this is not expected to significantly alter the conclusions because the build-up of mass in the simulations is independent of the group finder.

When combined with the link between the mass function and halo creation rate described in Percival *et al.* (2000), this leads to the interesting result that the cosmological change in the proportion of halos that have undergone recent merger is predicted to be independent of power spectrum, halo mass, mass function, and to only depend on the Friedmann cosmology through $d\delta_c/dt$. In Section 8 it was argued that the field galaxy merger rate should be driven by the halo merger rate, and that observations of field galaxies estimate the cosmological evolution in the halo merger rate. In Section 8, recent observational data were shown to be consistent with the presently favoured Λ CDM cosmology, although they are insufficiently accurate to usefully distinguish between cosmological parameters. It is hoped that future studies of this evolution will provide sufficiently accurate results that this picture will change.

10 ACKNOWLEDGEMENTS

I would like to thank John Peacock and the anonymous referee for useful comments that helped to improve this paper. The Hydra N-body code (Couchman, Thomas & Pearce 1995) was kindly made available by the Hydra consortium.

REFERENCES

- Abraham R.G., 1998, ‘Galaxy Interactions at Low and High Redshifts’, eds Barnes J.E., Sanders D.B., IAU Symp., 186, 11
 Barnes J.E., Hernquist L., 1992, ARA&A, 30, 705
 Bond J.R., Cole S., Efstathiou G., Kaiser N., 1991, ApJ, 379, 440
 Bower R.G., 1991, MNRAS, 248, 332
 Carlberg R.G., Pritchett C.J., Infante L., 1994, ApJ, 435, 540
 Couchman H. M. P., Thomas P.A., Pearce F.R., 1995, ApJ, 452, 797
 Jenkins A., Frenk C.S., White S.D.M., Colberg J.M., Cole S., Evrard A.E., Couchman H.M.P., Yoshida N., 2001, MNRAS, 321, 372
 Kauffmann G., White S.D.M., 1993, MNRAS, 261, 921
 Lacey C., Cole S., 1993, MNRAS, 262, 627
 Lacey C., Cole S., 1994, MNRAS, 271, 676
 Lavery R.L., Seitzer P., Suntzeff N.B., Walker A.R., Da Costa G.S., 1996, ApJ, 467, L1
 Le Fèvre O., *et al.*, 2000, MNRAS, 311, 565
 Neuschaefer L.W., Im M., Ratnatunga K.U., Griffiths R.E., Casertano S., 1997, ApJ, 480, 59
 Patton D.R., Pritchett C.J., Yee H.K.C., Ellington E., Carlberg R.G., 1997, ApJ, 475, 29
 Peacock J. A., Heavens A. F., 1990, MNRAS, 243, 133
 Percival W.J., Miller L., 1999, MNRAS, 309, 823
 Percival W.J., Miller L., Peacock J.A., 2000, MNRAS 318, 273
 Press W., Schechter P., 1974, ApJ, 187, 425
 Sheth R.K., Lemson G., 1999, MNRAS, 305, 946
 Sheth R.K., Tormen G., 1999, MNRAS, 308, 119
 Sheth R.K., Mo H.J., Tormen G., 2001, MNRAS, 323, 1
 Somerville R.S., Kolatt T.S., 1999, MNRAS, 305, 1
 Somerville R.S., Lemson G., Kolatt T.S., Dekel A., 2000, MNRAS, 316, 479